Deterministic Folding in Stiff Elastic Membranes

T. Tallinen,[1] J. A. Åström,[2] and J. Timonen[1]
[1]Department of Physics, P.O. Box 35, FI-40014 University of Jyväskylä, Finland
[2]Helsinki University of Technology, LCE, P.O. Box 9203, FI-02015 TKK, Finland
(Received 28 February 2008; published 2 September 2008)

Crumpled membranes have been found to be characterized by complex patterns of spatially seemingly random facets separated by narrow ridges of high elastic energy. We demonstrate by numerical simulations that compression of stiff *elastic* membranes with small randomness in their initial configurations leads to either random ridge configurations (high entropy) or nearly deterministic folds (low elastic energy). For folding with symmetric ridge configurations to appear in part of the crumpling processes, the crumpling rate must be slow enough. Folding stops when the thickness of the folded structure becomes important, and crumpling continues thereafter as a random process.

DOI: 10.1103/PhysRevLett.101.106101 PACS numbers: 68.60.Bs, 05.70.Np, 46.25.−y, 82.20.Wt

The crumpling of thin membranes is a common daily phenomenon, but it also has, on microscopic scales, interesting biological applications in, e.g., lipid membranes, vesicles, and virus capsids. Experiments are obviously much easier to do on thin sheets of common materials [1–5] in macroscopic scales, and they can be used to search for generic properties independent of the material or the scale. Crumpling a thin membrane so as to fit a confined volume has obviously a very large number of possible solutions. Crumpling of two similar sheets of paper will practically always result in two different crumpled configurations. It means that a crumpled sheet is in a state of high entropy, and two similar crumpled configurations cannot be found. This is consistent also with the crumpling experiments referred to above, and with simulation results [6–10]. Even though crumpled sheets are in a state of high entropy, not all possible fold patterns appear with equal possibility. In a slow enough deformation of an elastic body, configurations with low elastic energy are more likely to appear. Slow crumpling of a membrane can thus be considered as a ''competition'' between states of high entropy and low energy.

It would be very difficult to determine the distribution of crumpled structures of an elastic membrane as it would require determination of the entire energy landscape of the possible configurations of the membrane. Such an energy landscape is expected to be very complicated. In most experimental situations it is also not possible to explore that landscape because friction and/or plastic deformation effectively hinder the membrane to continuously change its configuration under crumpling so as to relax towards configurations of minimal elastic energy.

Using numerical simulations it is, however, easy to consider elastic membranes without friction and with no possibility of plastic deformations. We can thus address the question of whether crumpling of such a membrane is indeed dominated by entropy or is it at least partly dominated by only a few energetically favorable fold patterns. We demonstrate here that initially flat elastic membranes compactify with fairly equal probabilities into random crumpled configurations of high elastic energy and highly symmetric folded configurations of low elastic energy, when confined inside a spherical shell of slowly decreasing radius and there is no friction. The final configurations are very sensitive to initial conditions, but, at the same time, distinctly different initial conditions may lead to very similar final configurations.

To simulate the crumpling of a membrane we use a discrete-element method. Our simulation model consists of a triangular lattice with lattice spacing a and sites connected by massless beams with bending, shear, and tensile stiffness. These beams are viscoelastic Timoshenko beams [11] with a large rotation formulation [12]. They have width a, Young's modulus Y_b, and Poisson ratio $\nu = \frac{1}{3}$. Self-avoidance of the membrane is introduced via an elastic frictionless sphere with radius $a/2$, mass m, and Young's modulus $Y_s = Y_b$ at each lattice site. Only spheres beyond nearest neighbors are allowed to interact in order to avoid affecting the in-plane compressibility of the membrane. The full dynamics of the system is simulated by solving Newton's equations of motion.

In our simulations a rectangular membrane was placed inside a spherical shell of decreasing radius R, as shown in Fig. 1(a). Perturbations to the initial configurations were introduced by random variations in the initial height coordinate at each lattice site. These variations were chosen such that all deformation wavelengths were present, and the magnitude of each variation was proportional to its related wavelength. The maximum variation was of the order of membrane thickness. Other ways to introduce randomness (random forces and different magnitudes of height-coordinate variations) were also tested without qualitative changes in the results.

The behavior of the membrane is characterized by the width to thickness ratio $\lambda = L/h$ ($h \approx a$) and the ratio of elastic to inertial forces $\xi = Y/\rho u^2$, where ρ is the mass

 © 2008 The American Physical Society

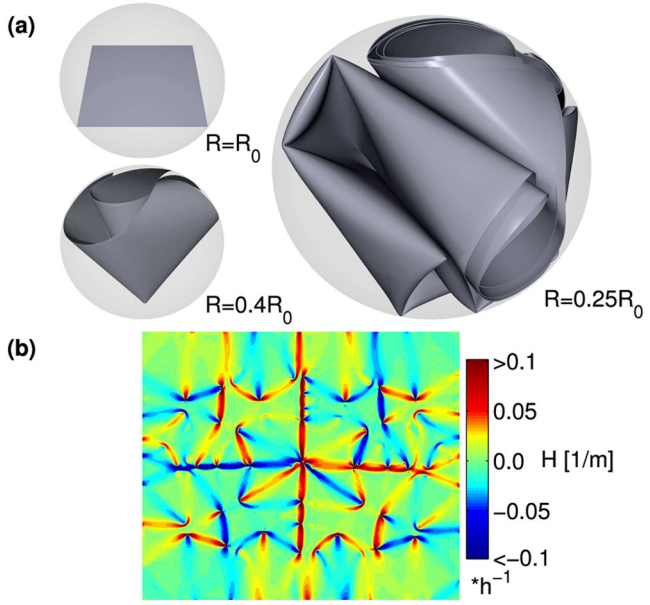

FIG. 1 (color online). A thin membrane folding inside a spherical shell. (a) Snapshots from simulations showing the initial configuration, the membrane deformed into a cone, and the membrane in a symmetrically folded configuration. (b) A color-coded mean curvature map of a folded configuration for $R = 0.25R_0$, which displays a symmetrical fold pattern. The width to thickness ratio of the membrane is 1000:1.

density of the material and u is the crumpling rate (the rate at which R is decreased). In the simulations we used λ up to 10^3, which is comparable to, e.g., sheets of paper and several types of biological membrane [13]. For ξ we used $\xi \approx 10^9$ which is a value big enough for inertial effects to be negligible and comparable to the rate at which a piece of paper is crumpled by hand.

We validated our model by comparing the stiffness of a flat membrane to that of a thin solid plate with the same parameters modeled by a standard finite element method. The tensile, shear, and bending stiffnesses were found to be in good agreement. We also compared the elastic energy of a simulated crumpled membrane with the expression $E \approx \int dS[\frac{1}{2}\kappa(\mathrm{Tr}\mathbf{C}_{ij})^2 + \frac{3}{16}Yh(\mathrm{Tr}\gamma_{ij})^2 + \frac{3}{8}Yh\mathrm{Tr}(\gamma_{ij})^2]$, introduced previously for the energy of a deformed membrane [14,15]. Here κ is the bending modulus of the membrane, and $\mathbf{C}_{ij}$ and γ_{ij} are the curvature and in-plane strain tensor, respectively, extracted from the lattice. We found again good agreement (within 30% in total energy) given that there are large local strains at vertices not accounted for by the above expression. We also implemented a model for thin membranes recently used in Refs. [9,16–18] and originally introduced by Seung [19]. This model is also based on a triangular lattice but, instead of beams, sites are connected by springs, and bending stiffness is produced by having an energy cost to bending of adjacent triangles of the lattice. While we expect that the beam model performs better for large local deformations, both models displayed very similar overall behavior during compression [20]. This is expected, since in sufficiently large sheets the fraction of the total energy related to large strains is very small, so the behavior is insensitive to the detailed form of the elastic potential.

In a crumpled membrane energy is concentrated in the conical vertices and the ridges between vertices (notice that *local* strains of beams in ridges are not necessarily very high as even a sharp bend is extended over many lattice spacings). Such structures have been extensively studied in Refs. [16,17,21–23]. A membrane confined in a small volume is thus expected to try to minimize the number of vertices and ridges within the constraints set by connectivity and self-avoidance. As the radius of the confining shell begins to decrease, the membrane is first deformed into a cone with only one sharp vertex. This deterministic deformation is observed also for, e.g., circular sheets confined in a sphere [9]. For $R < 0.4R_0$ the cone no longer fits the sphere, and new vertices and ridges are formed when it disappears.

In the formation of new vertices and ridges we observed two typical mechanisms: a vertex can bifurcate, and a ridge appears that connects the two vertices, or a nearly flat area can buckle and form a diamondlike pattern of ridges and vertices. The latter kind of structure appears, e.g., in buckling of a cylinder under a compressive lateral force, and has also been studied in the case of ridges [18]. Buckling and splitting of vertices appear to be more or less random after the cone breaks, and deformations become constrained by self-avoidance. Evidently self-avoidance easily "traps" the membrane in a local energy minimum making further relaxation difficult. Since we consider fully elastic membranes, existing vertices and ridges may, however, move without energy cost. This kind of "global relaxation" allows the membrane to compactify more efficiently with subsequent deformation with fewer vertices and ridges. This is the mechanism behind the symmetric folds that can appear under compression.

The possible configurations of crumpled membranes can roughly be divided into three categories according to the symmetry of fold pattern. Some membranes display configurations with no symmetric folds, as those in Figs. 2(a) and 2(b). Such configurations have high elastic energy, and the density of ridges and vertices is also high. Configurations also appear with a single symmetry axis in the middle of the membrane, as in Figs. 2(c) and 2(d). Such a membrane takes the form of a double layer that allows for larger facets and lower elastic energy, but thereafter crumpling appears to be random. The third category consists of membranes with two or more symmetric folds, which results in multilayer structures (up to 16 layers in our simulations), as shown in Figs. 1, 2(e), and 2(f). These membranes have considerably larger facets and thus much lower energy than randomly crumpled membranes [see also Figs. 3(e) and 3(f)]. In our simulations (a few dozen

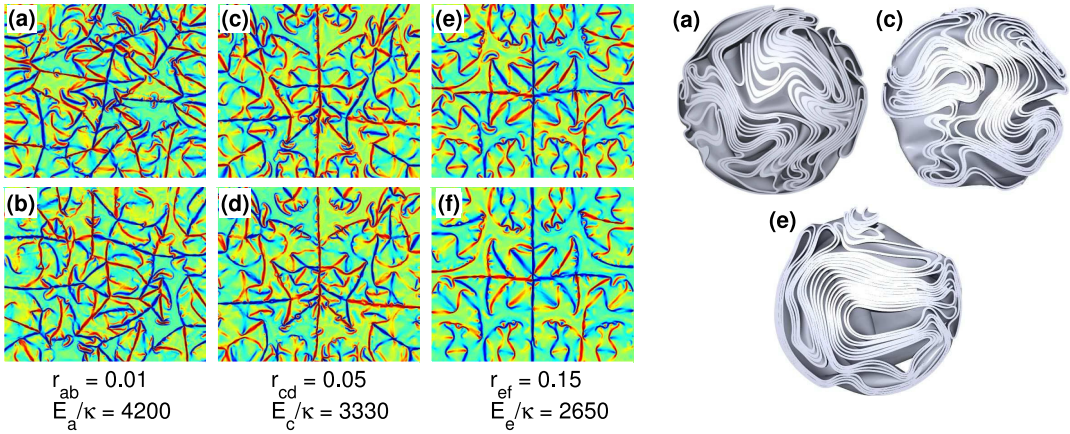

FIG. 2 (color online). (a),(b) Ridge patterns of configurations with no symmetric folds and very little cross correlation, $r_{ab} = 0.01$, between the patterns. (c),(d) Ridge patterns of configurations with one clearly symmetric fold. Cross correlation, $r_{cd} = 0.05$, is now increased compared to the previous cases (a),(b). (e),(f) Ridge patterns of configurations with two or more symmetric folds and a cross correlation of $r_{ef} = 0.15$. In all these membranes $\lambda = 500$, $R = 0.13R_0$, and the solid volume fraction is 0.5. The cross-section cuts on the right illustrate differences between the structures.

cases) all three categories appeared with roughly equal frequencies. Even very small changes in the initial configuration of the membrane typically resulted in a completely different final configuration. On the other hand, the membranes that showed very symmetric folding had almost identical ridge patterns even though their initial conditions were quite different. For different L/h we found very similar sets of ridge patterns, which held until the solid volume fractions of the compressed systems were more than about a third.

Cross correlations of the ridge patterns in membranes without symmetric folds (cf. Fig. 2, $r_{ab} = 0.01$) showed no signs of similarity. In contrast with this, the ridge patterns in the membranes with symmetric folds were clearly correlated (cf. Fig. 2, $r_{ab} = 0.15$). The most efficient way to decrease the dimensions of a membrane while creating as little ridge length as possible is to fold it as in Figs. 2(e) and 2(f). Such configurations have low configurational entropy and low elastic energy.

Next we studied in more detail how the facet size, ridge length, and elastic energy change during crumpling. If a membrane is compacted by repeated folding along a central line, the characteristic facet size X decreases linearly with the diameter of the confining shell, i.e., $X \sim R$. For random crumpling the facet size is expected to decrease faster. To extract the facet size and ridge length we determined the average linear size of areas with the same sign of curvature. After the single cone has disappeared ($R < 0.4R_0$), this size is also related to the characteristic linear size of the facets, which is proportional to the characteristic ridge length.

Figure 3(c) shows the characteristic facet size as a function of radius R for a membrane that undergoes folding before crumpling. A folding regime is visible for $0.4R_0 > R > 0.23R_0$ with two tight folds resulting in a compact four-layer structure. Thereafter the twice-folded membrane folds two more times, resulting in a loose 16-layer structure, as in Fig. 1(a). As a result of folding, the facet size remain similar to the radius of the confining shell. For $R < 0.23R_0$ the 16-layer stack is too wide to fit the sphere, but it is also too thick to fold further, and, consequently, no symmetric folds appear. There is a transition from symmetric folding to crumpling. This transition can be seen in Fig. 3(c), where the characteristic facet size begins to decrease more rapidly due to buckling of large facets. A snapshot of the transition regime is shown in Figs. 3(a) and 3(b).

During compression, fluctuations in the characteristic facet size are expected due to buckling events and other rapid changes in the membrane structure. Compared with the characteristic facet size, the elastic energy of the membrane changes smoothly. In Fig. 3(d) the characteristic facet size of a folding membrane is related to its elastic energy. The number of ridges in a membrane of width L can be approximated by $(L/X - 1)^2$, and the energy of a single ridge as $E_X/\kappa \approx \phi^{7/3}(X/h)^{1/3}$ [16,22], where ϕ is the complement to the angle between the two sides of a ridge. Multiplying these two quantities and substituting $\phi^{7/3} = 4.8$ (corresponding to a typical ridge angle, $\phi \approx 0.6\pi$), an estimate for the total energy of the system can be found. After the folding regime the characteristic facet size decreases quickly without a corresponding increase in the elastic energy. This is due to sharp ridges of high energy in the folds. When a folded stack buckles, sharp ridge angles open up, and the energy thereby released is used to form new ridges, cf. Fig. 3(b). This kind of interplay between the amount of ridges and their sharpness was found to be a generic feature in the simulations, and seems to be an important ingredient in conformation changes.

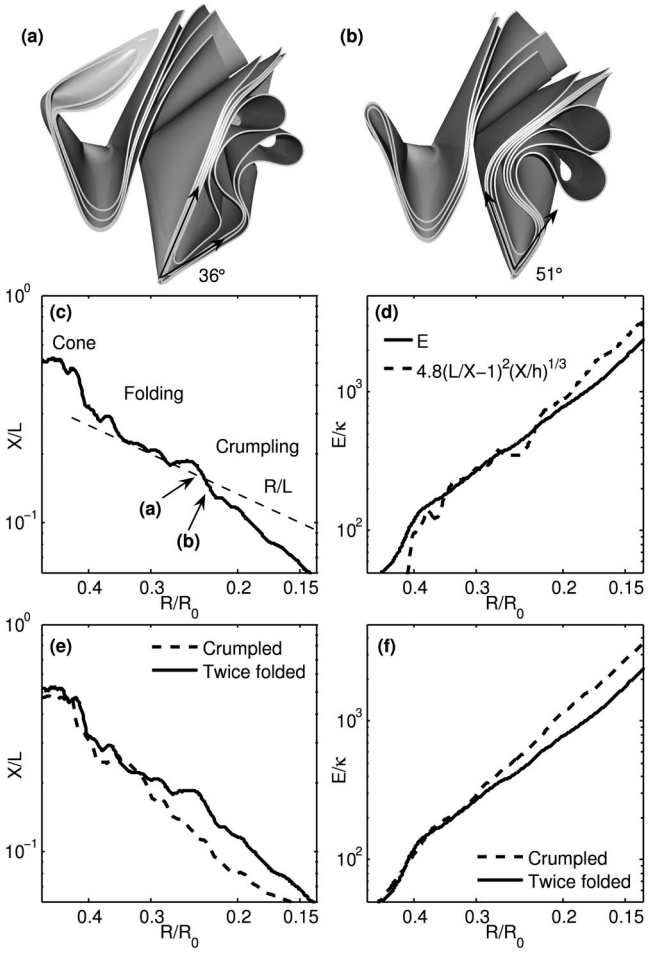

FIG. 3. (a),(b) Cross-section snapshots near transition from folding to crumpling [their location is indicated in (c)]. In (a) $R = 0.23R_0$ and the angle of a sharp ridge is 36°. In (b) $R = 0.22R_0$ and the same angle is considerably larger (51°). (c) The characteristic facet size (X/L) as a function of R/R_0 for the membrane in (a),(b). The regimes for conical configuration, folding, and crumpling are shown, and the facet size X/L is compared to the radius R/L of the configuration. (d) The related elastic energy (E) as a function of R/R_0. The energy estimated from the facet size X/L is also shown. In (e) and (f) comparison is made between the characteristic facet size and energy of the twice folding membrane of (a)–(d) and a membrane undergoing only random crumpling.

The rate of increase in energy for sheets undergoing folding was slightly less than that found in Ref. [9] and in the experiments of Ref. [1], where the energy scaling of crumpled membranes was found to be $E \sim R^{-3}$ and equivalent to $E \sim R^{-3.2}$, respectively. These rates of energy increase are, however, close to what we found for cases of no symmetric folds, which indicates that the membranes of Refs. [1,9] were only crumpled.

In summary, we have demonstrated that slow crumpling of elastic sheets without friction displays two qualitatively different modes of compression. Random crumpling with high entropy and deformation energy appears roughly as often as folded structures with low entropy and deformation energy. Folding does not seem to appear in sheets with friction and/or plastic deformation. For a sheet to fold, existing vertices and ridges must be able to move, allowing the sheet to globally change its shape and minimize its energy. Simulations display coexistence of folded and crumpled structures. This type of mode coexistence may allow, e.g., the observed wide variety of structures in biological membranes.

[1] K. Matan, R. B. Williams, T. A. Witten, and S. R. Nagel, Phys. Rev. Lett. **88**, 076101 (2002).
[2] D. L. Blair and A. Kudrolli, Phys. Rev. Lett. **94**, 166107 (2005).
[3] A. S. Balankin, R. C. M. de Oca, and D. S. Ochoa, Phys. Rev. E **76**, 032101 (2007).
[4] C. A. Andresen, A. Hansen, and J. Schmittbuhl, Phys. Rev. E **76**, 026108 (2007).
[5] M. A. F. Gomes, J. Phys. A **20**, L283 (1987).
[6] Y. Kantor, M. Kardar, and D. Nelson, Phys. Rev. Lett. **57**, 791 (1986).
[7] E. M. Kramer and T. A. Witten, Phys. Rev. Lett. **78**, 1303 (1997).
[8] J. A. Åström, J. Timonen, and M. Karttunen, Phys. Rev. Lett. **93**, 244301 (2004).
[9] G. A. Vliegenthart and G. Gompper, Nature Mater. **5**, 216 (2006).
[10] E. Sultan and A. Boudaoud, Phys. Rev. Lett. **96**, 136103 (2006).
[11] S. P. Timoshenko, *Strength of Materials* (Krieger Publishing, Huntington, NY, 1976).
[12] M. A. Crisfield, Comput. Methods Appl. Mech. Eng. **81**, 131 (1990).
[13] D. Nelson, T. Piran, and S. Weinberg, *Statistical Mechanics of Membranes and Surfaces* (World Scientific, Singapore, 2004), 2nd ed.
[14] T. A. Witten, Rev. Mod. Phys. **79**, 643 (2007).
[15] L. D. Landau and E. M. Lifshitz, *Theory of Elasticity* (Pergamon Press, Oxford, 1970).
[16] A. Lobkovsky, S. Gentges, D. Morse, H. Li, and T. A. Witten, Science **270**, 1482 (1995).
[17] T. Liang and T. A. Witten, Phys. Rev. E **73**, 046604 (2006).
[18] B. A. DiDonna and T. A. Witten, Phys. Rev. Lett. **87**, 206105 (2001).
[19] H. S. Seung and D. R. Nelson, Phys. Rev. A **38**, 1005 (1988).
[20] See EPAPS Document No. E-PRLTAO-101-033836 for a figure illustrating similar behavior under crumpling for sheets based on different elastic models. For more information on EPAPS, see http://www.aip.org/pubservs/epaps.html.
[21] T. Mora and A. Boudaoud, Europhys. Lett. **59**, 41 (2002).
[22] A. Boudaoud, P. Patricio, Y. Couder, and M. BenAmar, Nature (London) **407**, 718 (2000).
[23] E. Cerda, S. Chaieb, F. Melo, and L. Mahadevan, Nature (London) **401**, 46 (1999).